Available online at www.sciencedirect.com

SciVerse ScienceDirect

Ceramics International 39 (2013) 2631–2637

CERAMICS INTERNATIONAL

www.elsevier.com/locate/ceramint

Enhanced stability in CO_2 of Ta doped $BaCe_{0.9}Y_{0.1}O_{3-\delta}$ electrolyte for intermediate temperature SOFCs

A. Radojković[a,*], M. Žunić[a,b], S.M. Savić[a], G. Branković[a], Z. Branković[a]

[a]*Institute for Multidisciplinary Research, University of Belgrade, Kneza Višeslava 1a, 11030 Belgrade, Serbia*
[b]*Instituto de Química, UNESP–LIEC, CMDMC, Rua Prof. Francisco Degni, 55, CEP 14800–900, Araraquara, SP, Brazil*

Received 17 July 2012; received in revised form 7 September 2012; accepted 8 September 2012
Available online 15 September 2012

Abstract

The influence of Ta concentration on the stability of $BaCe_{0.9-x}Ta_xY_{0.1}O_{3-\delta}$ (where $x=0.01$, 0.03 and 0.05) powders and sintered samples in CO_2, their microstructure and electrical properties were investigated. The ceramic powders were synthesized by the method of solid state reaction, uniaxially pressed and sintered at 1550 °C to form dense electrolyte pellets. A significant stability in CO_2 indicated by the X-ray analysis performed was observed for the samples with $x \geq 0.03$. The electrical conductivities determined by impedance measurements in the temperature range of 550–750 °C and in various atmospheres (dry argon, wet argon and wet hydrogen) increased with temperature but decreased with Ta concentration. The highest conductivities were observed in the wet hydrogen atmosphere, followed by those in wet argon, while the lowest were obtained in the dry argon atmosphere for each dopant concentration. The composition with Ta content of 3 mol% showed satisfactory characteristics: good resistance to CO_2 in extreme testing conditions, while a somewhat reduced electrical conductivity is still comparable with that of $BaCe_{0.9}Y_{0.1}O_{3-\delta}$.

Keywords: A. Powders: solid state reaction; C. Electrical properties; D. Perovskites

1. Introduction

Proton conduction in materials with a perovskite structure such as barium cerate has been thoroughly studied in order to elucidate various issues on this phenomenon. It was found that barium cerate exhibits good ionic conductivity at raised temperatures only when doped with small amounts of trivalent cations (M^{3+}) similar in size with Ce^{4+} [1–10]. They occupy Ce sites in the lattice forming microstructure point defects, i.e. oxygen vacancies

$$Ce_{Ce}^{x}\,1/2O_{O}^{x} + 1/2M_2O_{3(s)} \rightarrow MC'_{Ce} + 1/2VO^{\bullet\bullet} + CeO_{2(s)} \quad (1)$$

In wet media the protons are incorporated into the lattice by water vapor uptake as described by the following mechanism [2–5,8,9,11–16]:

$$H_2O_{(g)} + V_O^{\bullet\bullet} + O_O^x \Leftrightarrow 2OH_O^{\bullet} \quad (2)$$

A relatively small amount of energy (~0.4 eV) is necessary for proton hopping from one oxygen ion to an adjacent one, causing a considerably high proton conductivity at elevated temperatures. Since the reaction described by Eq. (2) is exothermal [2,8,12–15], proton conduction is dominant usually in the temperature range from 500 °C to 700 °C [5–8,10,12]. Owing to its conductivity that reaches values up to $\sim 10^{-2}$ S/cm at 650 °C in a wet hydrogen atmosphere, $BaCe_{0.9}Y_{0.1}O_{3-\delta}$ (BCY) has been recognized as one of the best proton conducting electrolytes applicable in IT-SOFC systems [5,9,10,17,18].

However, the main drawback of BCY is its chemical stability, particularly in media rich in CO_2 at raised temperatures. As the material starts to decompose according to the following equation [16,19–21,23]:

$$BaO_{(\text{in BCY})} + CO_{2(g)} \Leftrightarrow BaCO_{3(s)} \quad (3)$$

a negative effect of the secondary phases on both the microstructure and the electrical properties of BCY will reduce the effectiveness of a fuel cell system. This can limit its usage in applications where CO_2 appears as a product,

*Corresponding author. Tel.: +381 11 2085037; fax: +381 11 2085038.
E-mail address: aleksandarrr@imsi.bg.ac.rs (A. Radojković).

0272-8842/$ - see front matter © 2012 Elsevier Ltd and Techna Group S.r.l. All rights reserved.
http://dx.doi.org/10.1016/j.ceramint.2012.09.028

mainly in SOFCs that use hydrocarbons as fuel [16,21]. According to the Lewis acid–base theory in solid oxide systems the basicity at O of the metal–oxygen bond increases with the increase of the electropositive character and the ionic radius of the metal [24]. In this respect, doping of BCY with elements that are more electronegative and have larger ionic radii than Ce and Y could raise overall acidity of the lattice, i.e. enhance resistance against carbonatization induced by CO_2. It has been reported that BCY shows good stability when doped with elements that satisfy the latter requirement (Nb, Zr or In), although with an inevitable decline in electrical properties [5,10,16,23,25].

The dopant valence also plays an important role since it is directly related to the formation of oxygen vacancies as described by Eq. (1). Thus, in the case of pentavalent ions such as Nb^{5+} and Ta^{5+}, a decrease in concentration of oxygen vacancies may occur due to the following reaction [23,26]:

$$Ce_{Ce}^{x} + 1/2V_{O}^{\bullet\bullet} + 1/2M_2O_{5(s)} \rightarrow M_{Ce}^{\bullet} + 1/2O_{O}^{x} + CeO_{2(s)} \quad (4)$$

Hence, it is reasonable to dope BCY with considerably lower concentrations of Ta than Y in order to prevent a significant decline in electrical properties. It has been previously shown that Ta enhanced the stability of $BaCe_{0.8}Y_{0.2}O_{3-\delta}$ in CO_2 [22], but only a single concentration of Ta (10 mol%) was investigated. Therefore, in this work BCY was doped with concentrations of Ta^{5+} up to 5 mol%, with the aim to determine the optimal concentration of Ta that will satisfy the criteria for both good electrical properties and stability in CO_2.

2. Experimental

2.1. Synthesis and processing of the ceramic powders

Synthesis of $BaCe_{0.9-x}Ta_xY_{0.1}O_{3-\delta}$ (where $x=0.01$, 0.03 and 0.05) powders, denoted as BCTY1, BCTY3, and BCTY5, was carried out by the solid state reaction method. Barium(II)-carbonate (Merck, Darmstadt, Germany), cerium(IV)-oxide (Carlo Erba, Milano, Italy), yttrium(III)-oxide (Merck, Darmstadt, Germany) and tantalum(V)-oxide (Merck, Darmstadt, Germany) were mixed with a small amount of 2-propanol (LACH-NER, s.r.o., Brno, Czech Republic) and homogenized for 24 h in a planetary ball mill using a tungsten carbide jar and balls. The mixture was dried at 50 °C for 2 h and ground in an agate mortar before being calcined at 1000 °C for 5 h. The resulting single-phased ceramic powders were uniaxially pressed into pellets 8 mm in diameter before being sintered in a tube oven at 1550 °C for 5 h.

2.2. Characterization of the powders and sintered samples

The powders were characterized by differential scanning calorimetry–thermogravimetric analysis (DSC–TGA; SDT Q600 V7.0 Build 84, TA Instruments, USA), X-ray diffraction (XRD; RIGAKU® RINT 2000, Tokyo, Japan) analysis and field-emission scanning electron microscopy (FESEM; JEOL JSM-6700F, Jeol Ltd., Tokyo, Japan). The microstructure of the sintered samples was investigated by scanning electron microscopy (SEM; TESCAN Vega TS5130MM, Tescan a.s., Brno, Czech Republic) and XRD analysis. The average grain size was estimated by the linear intercept method using at least three images of randomly selected surface areas.

Electrochemical impedance spectroscopy (EIS) was performed using a HIOKI 3532–50 LCR HiTESTER (HIOKI E. E. Corporation, Nagano, Japan) in a descending frequency mode from 1 MHz to 42 Hz. The thickness and diameter of the sintered pellets were as follows: BCTY1 (1.05 mm; 7.01 mm), BCTY3 (1.05 mm; 7.07 mm) and BCTY5 (0.97 mm; 6.95 mm). The samples were prepared by applying a Pt-paste on both sides of the pellets to form Pt/electrolyte/Pt symmetrical cells that were dried at 100 °C for 2 h before being treated for 30 min at 750 °C. Measurements were performed in the temperature range of 550–750 °C in a wet hydrogen (~3 vol% of H_2O), wet argon and dry argon atmosphere assuming the highest proton conduction in this temperature range. The wet atmospheres were provided by passing the gases through a gas washer filled with distilled water at room temperature. In the other case, the dry argon medium was secured with a gas trap filled with P_2O_5 mounted prior to the inlet of the cell system. The flow rate of the gases through the system was 50 cm^3/min and was kept constant by a digital mass flow controller and meter (MKS PR 4000B-F, MKS Instruments, Berlin, Germany).

2.3. Stability of the sintered ceramics in CO_2

The sintered samples were exposed to 100% CO_2 at 700 °C for 5 h in order to examine the degree of electrolyte decomposition as a function of Ta concentration. The heating and the cooling rates were 5 °C/min. After treatment in CO_2, changes in composition on the pellet surface were investigated by XRD analysis.

3. Results and discussion

3.1. Synthesis conditions and phase purity

In order to determine the solid state reaction temperature and secure complete decomposition of the starting barium carbonate during synthesis of $BaCe_{0.9-x}Ta_xY_{0.1}O_{3-\delta}$ (BCTY) powders, changes of the reaction mixture were tracked by DSC–TGA analysis up to 1400 °C. Fig. 1 shows DSC–TGA curves obtained for the BCTY3 powder. The endothermic peak present at slightly over 800 °C in the heat flow curve indicates a phase transformation in $BaCO_3$ [23,27]. The next endothermic trend with a maximum slightly below 1000 °C can be assigned to decomposition of barium carbonate with concomitant formation of the orthorhombic BCTY3 phase. This is followed by a maximal weight loss of approx. 8% on the derivative weight loss curve.

On the other hand, the XRD spectra of the BCTY powders calcined at 1350 °C, 1200 °C and 1000 °C show no presence of secondary phases. This confirms that a pure perovskite phase can be obtained even at 1000 °C, which can be seen in Fig. 2. Phase purity was also proved after sintering in air at 1550 °C for 5 h. The XRD spectra show only slightly sharper and more pronounced reflection lines that can be ascribed to a higher crystallinity degree of the sintered samples (Fig. 2).

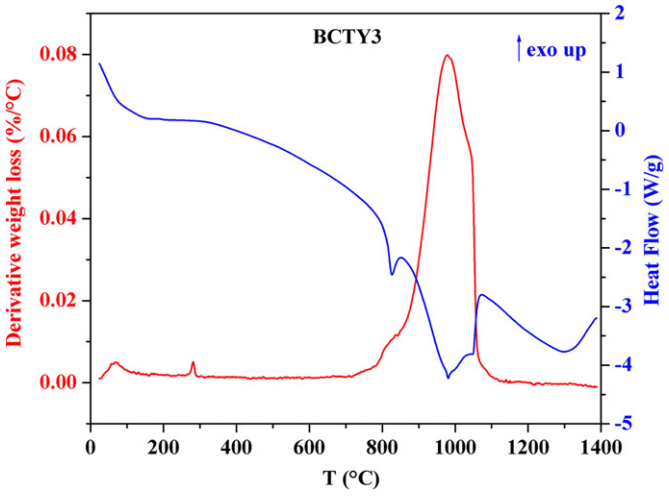

Fig. 1. DSC–TGA analysis of the BCTY3 sample.

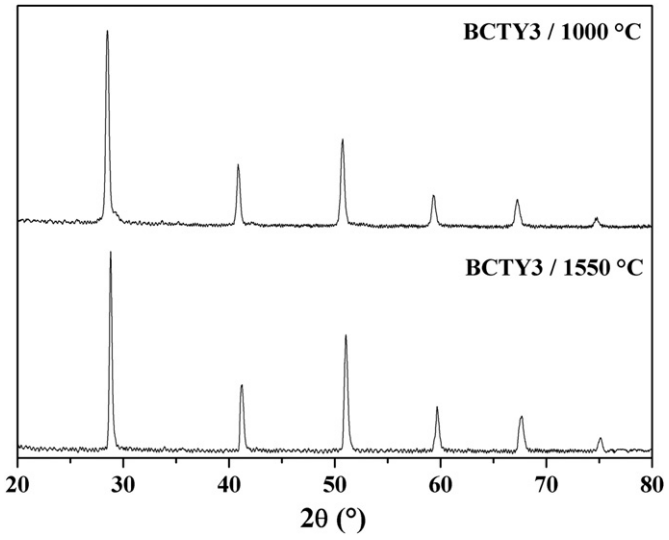

Fig. 2. XRD pattern of BCTY3 calcined at 1000 °C for 5 h and sintered at 1550 °C for 5 h.

3.2. Microstructure of the BCTY ceramics

Properties such as particle size distribution and agglomeration degree of ceramic powders have a strong influence on the resulting microstructure and properties of the sintered specimens [5–8,10,16]. FESEM images of the BCTY powders presented in Fig. 3 show similar microstructures with clusters of agglomerated particles up to a few hundreds of nanometers. The crystallite size, calculated from the Scherrer equation, was ~20 nm for all investigated samples showing no correlation between the Ta content and crystal growth. It is remarkable that even at 1000 °C the primary, grain-like particles have started to merge indicating the beginning of the sintering process.

SEM images of surfaces of samples sintered at 1550 °C are shown in Fig. 4. Dense microstructures with flat grain boundaries indicate that the sintering process has completed. All samples showed a bimodal grain size distribution. The most expressed was obtained for the BCTY5 sample. The average grain size slightly decreased with the increase of Ta content from 1.2 μm (BCTY1) to 1.0 μm (BCTY5). Values around 1 μm are typical for doped BCY [6,12,23,25], and the reduced grain growth in the case of Ta shows its negative effect on the sinterabilty of BCY ceramics as reported elsewhere [22,26]. Furthermore, since the samples with smaller grains contain more grain boundaries per volume unit, a decrease in their electrical conductivities could also be expected. An increase of the sintering temperature as a way to enhance grain growth is limited by evaporation of BaO that occurs above 1500 °C [3,6,7,19,21]:

$$BaCeO_{3(s)} \Leftrightarrow BaO_{(g)} + CeO_{2(s)} \quad (5)$$

This process deteriorates the microstructure of the electrolyte, eventually leading to worse electrical properties.

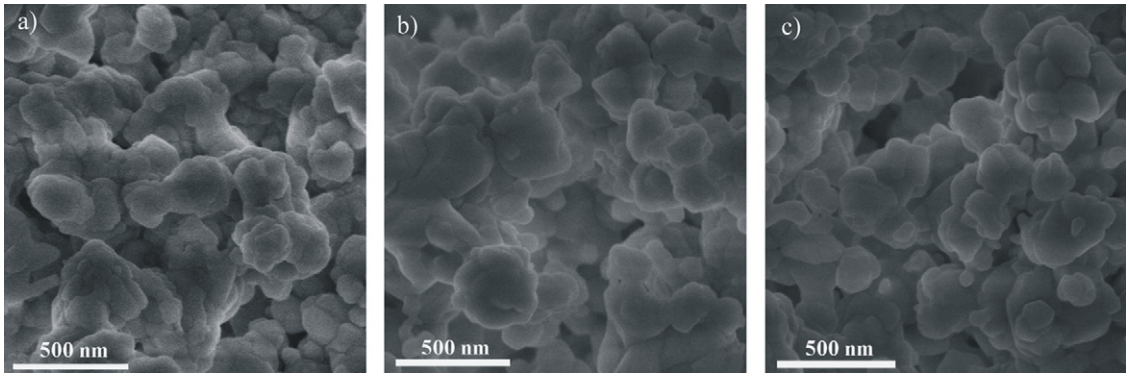

Fig. 3. FESEM images of powders calcined at 1000 °C for 5 h: (a) BCTY1, (b) BCTY3 and (c) BCTY5.

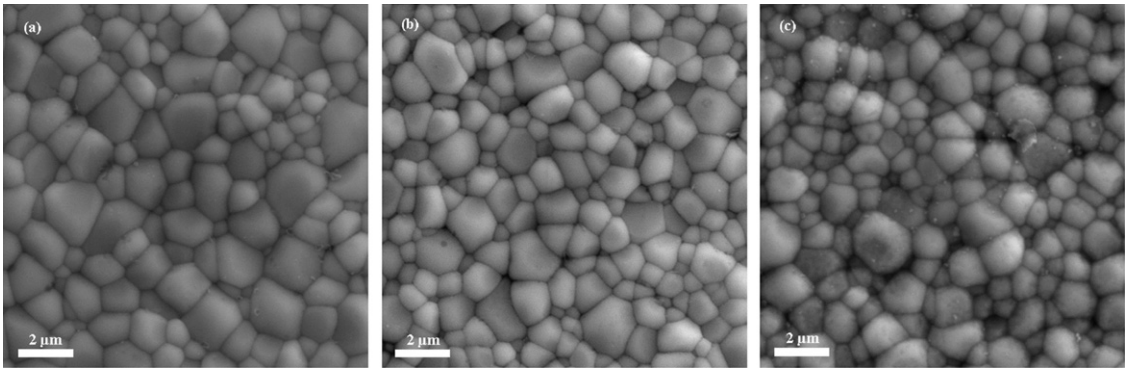

Fig. 4. SEM images of surfaces of samples sintered at 1550 °C for 5 h: (a) BCTY1, (b) BCTY3 and (c) BCTY5.

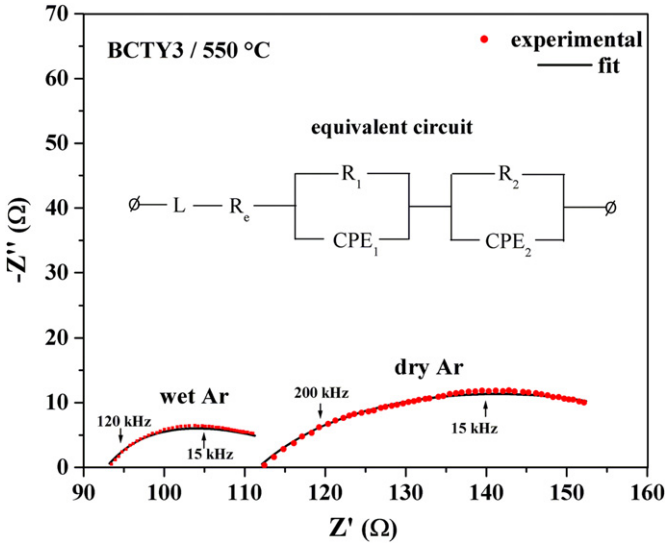

Fig. 5. Nyquist plots for BCTY3 in the wet and dry argon atmospheres at 550 °C.

3.3. Electrical properties of the BCTY electrolytes

Since BCY is applicable in IT-SOFC systems, impedance analysis was performed in the temperature range between 550 °C and 750 °C. However, at these temperatures it was not possible to distinguish between grain boundary and grain interior contributions to the total sample resistivity, except only at 550 °C in the wet and dry argon atmospheres. In the wet hydrogen atmosphere the grain boundary arc almost completely disappeared even at 550 °C and it could not be modeled with certainty. In Fig. 5 Nyquist plots of BCTY3 are shown at 550 °C in wet and dry argon atmospheres. Curve fitting was performed using the EIS Spectrum Analyzer Software. Stray inductance, L, resistors: R_e, R_1, R_2 and constant phase elements, denoted as CPE_1 and CPE_2 were used as elements of the equivalent circuit. The two constant phase elements were related to the two almost merged semicircles. The first arc at higher frequencies refers to grain boundaries (CPE_1), while the second one is related to charge transfer processes at the electrode/electrolyte interface (CPE_2). The real grain boundary capacitance, C, was calculated using the following expression [6,7,19,23]:

$$C = R^{1-n/n} Q^{1/n} \tag{6}$$

where Q and n represent the parameters of the constant phase elements and R is the resistivity of the grain boundary. The capacitance values obtained for the BCTY3 sample were 1.1×10^{-9} F/cm in wet argon and 3.0×10^{-9} F/cm in dry argon, whereby 10^{-9} F/cm is an order of magnitude typical for grain boundary capacitance [6,7,13,16,23]. This difference in grain boundary capacitance is followed by a difference in grain boundary resistivity at 550 °C (106.1 Ω in dry Ar and 73.4 Ω in wet Ar). The oxygen vacancies tend to pile up in a grain boundary core minimizing the energy of the angular mismatch between crystalline lattices of adjacent grains [28]. This positive grain boundary core together with a neighboring negative space-charge layer is characterized by a Schottky barrier height, which is responsible for higher grain boundary resistivities [29]. The lower value determined for grain boundary resistivity in the wet argon atmosphere can be explained by a higher mobility of proton defects originating from the hydration of oxygen vacancies as described by Eq. (2).

Activation energies (E_a) were calculated from Ahrrenius plots according to the derived equation:

$$\ln(\sigma T) = \ln A - \frac{Ea}{k}\frac{1}{T} \tag{7}$$

where σ is the conductivity, T is the absolute temperature, A is the pre-exponential factor and k is the Boltzmann constant. Total conductivities of the BCTY samples in the form the Ahrrenius plots are shown in Fig. 6. Their values depended on three parameters: temperature, concentration of Ta and atmosphere. By keeping any two of them constant, the total conductivities: (i) increase with temperature, (ii) decrease with concentration of Ta and (iii) decrease in the following order: $\sigma_{\text{wet hydrogen}} > \sigma_{\text{wet argon}} > \sigma_{\text{dry argon}}$. The determined activation energies varied around 0.4 eV and they slightly increase with the increase of Ta concentration. The value of 0.4 eV has been previously reported for BCY in wet hydrogen [23], while for doped BCY, E_a varies between 0.3 and 0.6 eV [6,10,25]. The highest values were observed in the dry argon

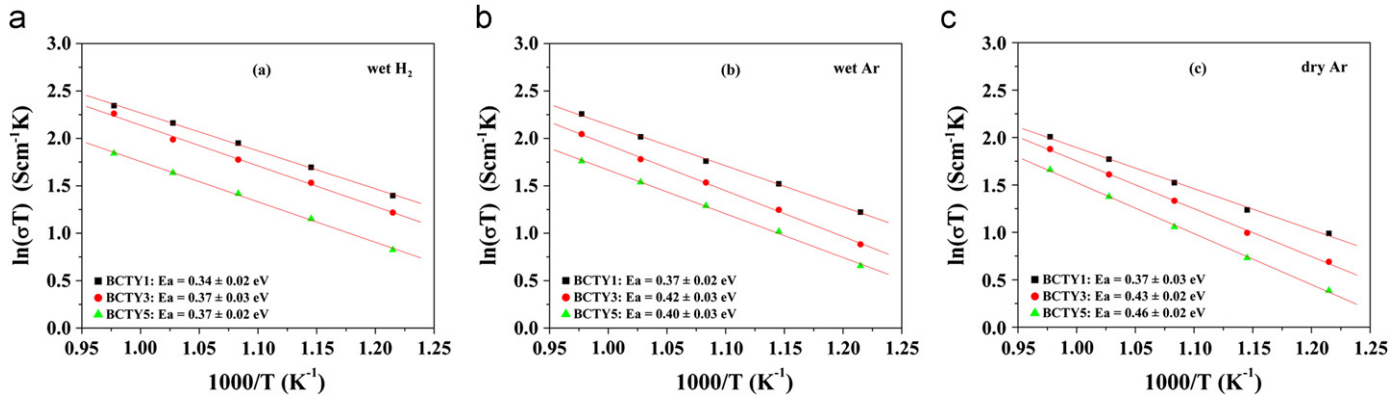

Fig. 6. Total conductivities of the BCTY samples in the form of Arrhenius plots in different media: (a) wet hydrogen, (b) wet argon and (c) dry argon.

atmosphere, followed by those in wet argon for each electrolyte composition. As the highest concentration of protons can be obtained in a wet hydrogen environment, it is reasonable to expect the highest conductivities along with the lowest activation energies in this medium. In environments with no source of protons such as dry Ar, the lowest conductivities were obtained due to conducting mechanisms that require higher activation energies [1,12,14,16]. In this case, oxygen ions and electron holes are the charge carriers taking part in the conducting mechanism. Electron holes can arise at higher oxygen partial pressures and at raised temperatures, in an environment such as during sintering in air [1,4,7,8,12,14,16]:

$$V_O^{\bullet\bullet} + 1/2O_{2(g)} \leftrightarrow O_O^x + 2h^{\bullet} \quad (8)$$

Although hydration of electron holes is less favorable than hydration of oxygen vacancies [28], in wet environments the conductivity contribution of electron holes is expected to be reduced due to water uptake according to the following equation:

$$H_2O_{(g)} + 2O_O^x + 2h^{\bullet} \rightarrow 2OH_O^{\bullet} + 1/2O_{2(g)} \quad (9)$$

Summarily, proton conduction in wet media is dominant at lower temperatures, while the oxygen ion conducting mechanism prevails at temperatures above 800 °C [4,28].

When it comes to the influence of Ta on electrical properties, the experimental results are in agreement with the assumptions made previously: a decrease in vacancy concentration (according to Eq. (4)) would result in a decreased conductivity. Besides, the activation energies show a tendency to increase with the increase of dopant concentration. This can be explained by a reduced mobility of charge carriers caused by a lattice distortion [6,7,25] when Ta^{5+} with a relatively small ionic radius (0.64 Å) occupies the site of Ce^{4+} (0.87 Å) in the BO_6 octahedra of the perovskite structure (ABO_3). Total conductivities in the wet hydrogen atmosphere as a function of Ta concentration and temperature are presented in Table 1 The electrolytes doped with 1 and 3 mol% of Ta still remain comparable to the undoped BCY with a drop in conductivity of ~35% for the BCTY3 composition at 650 °C.

Table 1
Total conductivities in the wet hydrogen atmosphere as a function of Ta concentration and temperature.

T (°C)	$\sigma \times 10^2$ (S/cm)		
	BCTY1	**BCTY3**	**BCTY5**
750	1.01 ± 0.01	0.94 ± 0.01	0.62 ± 0.01
700	0.89 ± 0.01	0.75 ± 0.01	0.53 ± 0.01
650	0.76 ± 0.01	0.64 ± 0.01	0.45 ± 0.01
600	0.62 ± 0.01	0.53 ± 0.01	0.36 ± 0.01
550	0.49 ± 0.01	0.41 ± 0.01	0.28 ± 0.01

A similar material has been already investigated as an electrolyte for IT-SOFC by Bi et al. [22] In their case conductivity of electrolyte was 0.23×10^{-2} S/cm^2 at 600 °C (0.53×10^{-2} S/cm^2 was observed for BCTY3 at the same temperature) and maximum power output obtained from fuel cell tests was 137 mW/cm^2.

3.4. Stability in CO_2

As stated in the introduction of this paper, the main disadvantage of BCY as an electrolyte for IT-SOFCs is its vulnerability to CO_2 at raised temperatures. The BCTY electrolytes were exposed to 100% CO_2 at 700 °C, an environment that is by far more extreme than the operating conditions of SOFCs using hydrocarbon based fuels or another, where CO_2 emanates as a product. This condition was chosen in order to assess the degree of stability as a function of Ta concentration in a shorter period of time (5 h), and it can be described as an accelerated stability test [21]. Fig. 7 shows the XRD spectra of the BCTY samples after treatment in 100% CO_2 atmosphere at 700 °C for 5 h. The presence of $BaCO_3$ and CeO_2 as secondary phases was detected in all spectra suggesting the reaction of BCTY decomposition

$$BaCeO_{3\ (BCTY)} + CO_{2\ (g)} \Leftrightarrow BaCO_{3(s)} + CeO_{2(s)} \quad (10)$$

This reaction can be conveniently described as a reaction of neutralization according to the Lux-Flood acid–base theory [30]. It is applicable to solid systems, stating that

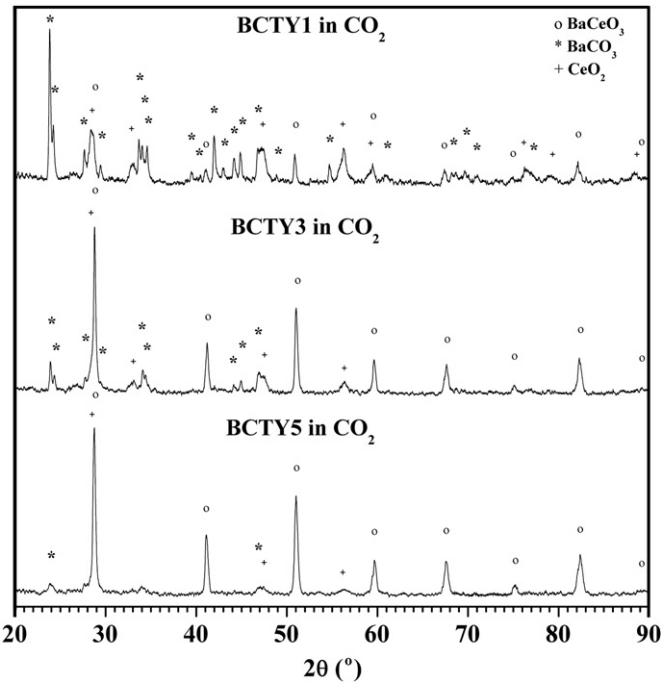

Fig. 7. XRD spectra of the BCTY samples after treatment in 100% CO_2 atmosphere at 700 °C for 5 h.

acids (CO_2) represent acceptors of oxygen ions, while bases (BaO) are their donors. To inhibit the reaction of BCY decomposition (neutralization), it is necessary to increase the acidity of O^{2-} ions in the perovskite structure, especially those bonded to barium. It may be possible to achieve this by introducing elements that are more electronegative than Ce, such as Ta, Nb or In into the lattice. As shown in Fig. 7, the most stable composition was achieved with the highest concentration of Ta (5 mol%). A significant resistance to CO_2 was also shown by BCTY3 considering the extreme conditions of the experiment. It is important to note that degradation of a dense electrolyte sample occurs mostly at its surface, and it can be even less expressed in electrolytes coated with electrodes [21].

4. Conclusion

The stability of doped BCY in CO_2, its microstructure and electrical properties, still remain one of the most important concerns that limit its utilization in IT-SOFCs applications. The influence of Ta doping on the properties of BCY is multiple: it decreases the average grain size of the sintered samples and the concentration of oxygen vacancies. On the other hand, it causes distortion of the crystal lattice. All these features lead to degradation of the electrical properties that were investigated in the temperature range of 550–750 °C regardless of atmosphere. In spite of that, the stability in CO_2 was enhanced with increased dopant levels as a consequence of the raised acidity of the crystal lattice. BCTY3 showed the most promising properties of the three compositions investigated in terms of considerable stability in CO_2 (taking into account the extreme testing conditions) and a relatively high conductivity in the wet hydrogen atmosphere at 650 °C (0.64×10^{-2} S/cm). The other two electrolytes showed either poor chemical stability (BCTY1) or unsatisfactory electrical properties (BCTY5).

Acknowledgments

The authors acknowledge that this work was supported by the Ministry of Education and Science of the Republic of Serbia (Project no. III45007) and Fundação de Amparo à Pesquisa do Estado de Saõ Paulo-FAPESP (Project no. 2010/20574–3). The authors also appreciate the valuable help of Jelena Miladinović and Dejan Poleti, professors at the Faculty of Technology and Metallurgy, University of Belgrade.

References

[1] T. Hea, K.D. Kreuer, Yu.M. Baikov, Impedance spectroscopic study of thermodynamics and kinetics of a Gd-doped $BaCeO_3$ single crystal, Solid State Ionics 95 (1997) 301–308.
[2] T. Norby, Solid-state protonic conductors: principles, properties, progress and prospects, Solid State Ionics 125 (1999) 1–11.
[3] A. Kruth, J.T.S. Irvine, Water incorporation studies on doped barium cerate perovskites, Solid State Ionics 162–163 (2003) 83–91.
[4] H. Iwahara, Ionic conduction in perovskite-type compounds, in: T. Ishihara (Ed.), Perovskite oxide for solid oxide fuel cells, Springer, Dordrecht, Heidelberg, London, New York, 2009, pp. 45–62.
[5] F. Zhao, Q. Liu, S. Wang, K. Brinkman, F. Chen, Synthesis and characterization of $BaIn_{0.3-x}Y_xCe_{0.7}O_{3-\delta}$ ($x=0$, 0.1, 0.2, 0.3) proton conductors, International Journal of Hydrogen Energy 35 (2010) 4258–4263.
[6] M. Amsia, D. Marrero-López, J.C. Ruiz-Morales, S.N. Savvin, M. Gabás, P. Núnez, Influence of rare-earth doping on the microstructure and conductivity of $BaCe_{0.9}Ln_{0.1}O_{3-\delta}$ proton conductors, Journal of Power Sources 196 (2011) 3461–3469.
[7] M. Amsif, D. Marrero-López, J.C. Ruiz-Morales, S.N. Savvin, P. Núnez, Effect of sintering aids on the conductivity of $BaCe_{0.9}Ln_{0.1}O_{3-\delta}$, Journal of Power Sources 196 (2011) 9154–9163.
[8] D. Medvedev, V. Maragou, T. Zhuravleva, A. Demin, E. Gorbova, P. Tsiakaras, Investigation of the structural and electrical properties of co-doped $BaCe_{0.9}Gd_{0.1}O_{3-\delta}$, Solid State Ionics 182 (2011) 41–46.
[9] T. Tauer, R. O'Hayre, J.W. Medlin, A theoretical study of the influence of dopant concentration on the hydration properties of yttrium-doped barium cerate, Solid State Ionics 204–205 (2011) 27–34.
[10] K. Gdula-Kasica, et al., Optimization of microstructure and properties of acceptor-doped barium cerate, Solid State Ionics (2012)http://dx.doi.org/10.1016/j.ssi.2012.04.022.
[11] T. Scherban, A.S. Nowick, Bulk protonic conduction in Yb-doped $SrCeO_3$, Solid State Ionics 35 (1989) 189–194.
[12] S. Ricote, N. Bonanos, G. Caboche, Water vapour solubility and conductivity study of the proton conductor $BaCe_{(0.9-x)}Zr_xY_{0.1}O_{(3-\delta)}$, Solid State Ionics 180 (2009) 990–997.
[13] T.S. Bjørheim, A. Kuwabara, I. Ahmed, R. Haugsrud, S. Stølen, T. Norby, A combined conductivity and DFT study of protons in $PbZrO_3$ and alkaline earth zirconate perovskites, Solid State Ionics 181 (2010) 130–137.
[14] C. Zhang, H. Zhao, Electrical conduction behavior of Sr substituted proton conductor $Ba_{1-x}Sr_xCe_{0.9}Nd_{0.1}O_{3-\delta}$, Solid State Ionics 181 (2010) 1478–1485.

[15] C. Kjølseth, L.-Y. Wang, R. Haugsrud, T. Norby, Determination of the enthalpy of hydration of oxygen vacancies in Y-doped $BaZrO_3$ and $BaCeO_3$ by TG-DSC, Solid State Ionics 181 (2010) 1740–1745.
[16] L. Bi, E. Fabbri, Z. Sun, E. Traversa, Sinteractivity, proton conductivity and chemical stability of $BaZr_{0.7}In_{0.3}O_{3-\delta}$ for solid oxide fuel cells (SOFCs), Solid State Ionics 196 (2011) 59–64.
[17] X.-T. Su, Q.-Z. Yan, X.-H. Ma, W.-F. Zhang, C.-C. Ge, Effect of co-dopant addition on the properties of yttrium and neodymium doped barium cerate electrolyte, Solid State Ionics 177 (2006) 1041–1045.
[18] S.B.C. Duval, P. Holtappels, U. Stimming, T. Graule, Effect of minor element addition on the electrical properties of $BaZr_{0.9}Y_{0.1}O_{3-\delta}$, Solid State Ionics 179 (2008) 1112–1115.
[19] K.H. Ryu, S.M. Haile, Chemical stability and proton conductivity of doped $BaCeO_3$–$BaZrO_3$ solid solutions, Solid State Ionics 125 (1999) 355–367.
[20] S. Yamaguchi, K. Nakamura, T. Higuchi, S. Shin, Y. Iguchi, Basicity and hydroxyl capacity of proton-conducting perovskites, Solid State Ionics 136–137 (2000) 191–195.
[21] N. Zakowsky, S. Williamson, J.T.S. Irvine, Elaboration of CO_2 tolerance limits of $BaCe_{0.9}Y_{0.1}O_{3-\delta}$ electrolytes for fuel cells and other applications, Solid State Ionics 176 (2005) 3019–3026.
[22] L. Bi, S. Zhang, S. Fang, Z. Tao, R. Peng, W. Liu, A novel anode supported $BaCe_{0.7}Ta_{0.1}Y_{0.2}O_{3-\delta}$ electrolyte membrane for proton-conducting solid oxide fuel cell, Electrochemistry Communications 10 (2008) 1598–1601.
[23] A. Radojković, et al., Chemical stability and electrical properties of Nb doped $BaCe_{0.9}Y_{0.1}O_{3-\delta}$ as a high temperature proton conducting electrolyte for IT-SOFC, Ceramics International (2012)http://dx.doi.org/10.1016/j.ceramint.2012.06.026.
[24] A. Zecchina, C. Lamberti, S. Bordiga, Surface acidity and basicity: general concepts, Catalysis Today 41 (1998) 169–177.
[25] E. Di Bartolomeo, A. D'Epifanio, C. Pugnalini, F. Giannici, A. Longo, A. Martorana, S. Licoccia, Structural analysis, phase stability and electrochemical characterization of Nb doped $BaCe_{0.9}Y_{0.1}O_{3-x}$ electrolyte for IT-SOFCs, Journal of Power Sources 199 (2012) 201–206.
[26] K. Xiea, J. Zhoua, G. Meng, Pervoskite-type $BaCo_{0.7}Fe_{0.2}Ta_{0.1}O_{3-\delta}$ cathode for proton conducting IT-SOFC, Journal of Alloys and Compounds 506 (2010) L8–L11.
[27] S.M. Antao, I. Hassan, $BaCO_3$: high-temperature crystal structures and the Pmcn → R3m phase transition at 811 °C, Physics and Chemistry of Minerals 34 (2007) 573–580.
[28] T. Norby, Proton conductivity in perovskite oxides, in: T. Ishihara (Ed.), Perovskite Oxide for Solid Oxide Fuel Cells, Springer, Dordrecht, Heidelberg, London, New York, 2009, pp. 217–238.
[29] C. Kjølseth, H. Fjeld, Ø. Prytz, P.I. Dahl, C. Estournès, R. Haugsrud, T. Norby, Space-charge theory applied to the grain boundary impedance of proton conducting $BaZr_{0.9}Y_{0.1}O_{3-\delta}$, Solid State Ionics 181 (2010) 268–275.
[30] H. Flood, T. Förland, The acidic and basic properties of oxides, Acta Chemica Scandinavica 1 (1947) 592–604.